Simulated annealing prediction of the crystal structure of ternary inorganic compounds using symmetry restrictions †

Luis Reinaudi,[a] Ezequiel P. M. Leiva[a] and Raúl E. Carbonio *[b]

[a] *INFIQC, Unidad de Matemática y Física, Facultad de Ciencias Químicas, Universidad Nacional de Córdoba, Ciudad Universitaria, 5000 Córdoba, Argentina*
[b] *INFIQC, Departamento de Fisicoquímica, Facultad de Ciencias Químicas, Universidad Nacional de Córdoba, Ciudad Universitaria, 5000 Córdoba, Argentina*

In this work we undertake a set of studies concerning the prediction of the structures of compounds of the type $ATiO_3$ (A = Sr, Ca, Ba) based only on the previous knowledge of the unit cell shape and content. We show that the interatomic potentials obtained for binary compounds (binary oxides AO and TiO_2 (rutile)) are very useful for the prediction of the structures of ternary compounds using simulated annealing with only the incorporation of the potential energy in the cost function. For these reasons, these simulations show the real possibilities of the method to predict the structures of compounds with previously unknown structures. A tremendous increase in the efficiency of obtaining the correct structure and in the accuracy of the atomic coordinates was obtained by the incorporation of space symmetry elements obtainable from powder diffraction.

1 Introduction

In the last decade, the prediction of the structure of inorganic solids from only the knowledge of its chemical composition and unit cell has become a great challenge.[1–5] The usual approach to this problem is to find the global minimum of a cost function that, in the case of inorganic solids, contains the potential energy of the system and some other additional constraints like comparison of the calculated and experimental diffraction patterns.[4]

We have previously shown that significant improvements can be achieved when space symmetry information obtainable from powder diffraction is used in the calculation of the structure of binary compounds.[1]

In the present work we undertake a set of studies concerning the prediction of the structures of compounds of the type $ATiO_3$ (A = Sr, Ca, Ba). Cubic $SrTiO_3$ (space group = $Pm3m$, $a = 3.95$ Å, $Z = 1$),[6] orthorhombic $CaTiO_3$ (space group = $Pnma$, $a = 5.38$, $b = 5.44$, $c = 7.639$ Å, $Z = 4$)[7] and hexagonal $BaTiO_3$ (space group = $P6_3/mmc$, $a = 5.724$, $c = 13.965$ Å, $Z = 6$)[8] were used. Even though hexagonal $BaTiO_3$ is not the stable phase at room temperature, it was chosen in order to have a growing complexity in the series $SrTiO_3 < CaTiO_3 < BaTiO_3$. The interest for these calculations arises from the fact that these compounds are ternary compounds of a relatively high complexity and that the potentials used for the simulations were obtained from other compounds (binary oxides AO and TiO_2 (rutile)). This shows the real possibilities of simulated annealing to predict unknown crystal structures of inorganic solids.

2 Preliminary calculations

Previous to the computer runs devoted to the prediction of the crystal structure, a set of preliminary studies was made in order to analyse the behaviour of the potentials to be used in the simulated annealing procedure. These studies involve the

Table 1 Short-range potential parameters used in the calculations (taken from refs. 13 and 14)

$V(r) = Ae^{-r/\rho} - Cr^{-6a}$	
A(Ti–O)/eV	754.2
ρ(Ti–O)/Å	0.3879
A(Sr–O)/eV	959.1
ρ(Sr–O)/Å	0.3721
A(Ca–O)/eV	1090.4
ρ(Ca–O)/Å	0.3437
A(Ba–O)/eV	905.7
ρ(Ba–O)/Å	0.3976
A(O–O)/eV	22764.3
ρ(O–O)/Å	0.1490
C(O–O)/eVÅ⁶	27.88

[a] $V(r)$ = short-range term of lattice energy; r = interatomic distance; ρ = adjustable parameter; A = adjustable parameter for the repulsive part of the short-range potential; C = adjustable parameter for the attractive part of the short-range potential.

calculation of the lattice energy, which was performed using an Ewald summation for the coulombic term and a real space evaluation of the short-range terms based on the Buckingham model. Formal charges were used (A^{2+}, Ti^{4+} and O^{2-}). Parameters of the short-range potential model are shown in Table 1.

Compressibility curves were calculated for these compounds in order to test whether the potentials could reproduce the experimental cell parameters. These curves were made by plotting the lattice energy (U) against the cell parameter (a). The three cell parameters (a, b and c) were varied so as to keep constant the ratio $a:b:c$. To calculate the energy, fractional atomic coordinates of the experimental structures were used. The results are shown in Fig. 1. The values (a_{calc}) that minimise the energy are shown in Table 2. The experimental values of cell parameters were reproduced within 2% for the three compounds.

Taking into account that the potentials used here were not fitted to the calculated compounds, it has to be expected that the crystal structure corresponding to the minimum energy does not correspond exactly to the experimental structure;

Table 2 Experimental (a_{exp}) and calculated from compressibility curves (a_{calc}) cell parameters for $SrTiO_3$, $CaTiO_3$ and $BaTiO_3$. For $CaTiO_3$ and $BaTiO_3$, only one parameter (a) is shown

	a_{exp}/Å	a_{calc}/Å	$(a_{calc} - a_{exp})/a_{exp}$
$SrTiO_3$	3.95	3.98	7.6×10^{-3}
$CaTiO_3$	5.38	5.47	1.7×10^{-2}
$BaTiO_3$	5.73	5.83	1.7×10^{-2}

Table 3 Comparison of lattice energies per formula obtained with crystallographic atomic positions (U_{cryst}), after relaxation to the closest energy minimum (U_{relax}) and calculated with a Born–Haber cycle (U_{B-H})

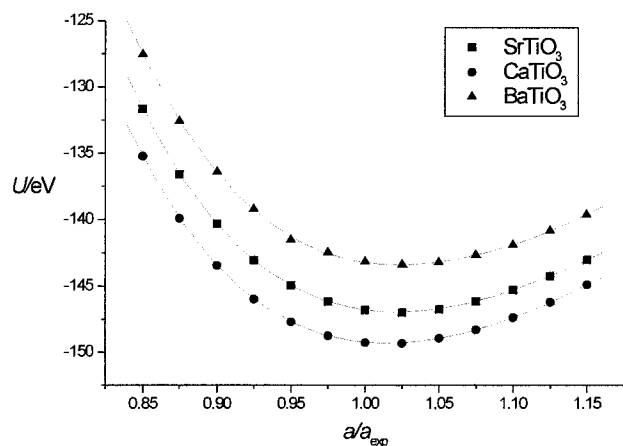|	U_{cryst}/eV	U_{relax}/eV	U_{B-H}/eV
$SrTiO_3$	−146.810	−146.810	−143.83
$CaTiO_3$	−149.275	−149.313	−143.23
$BaTiO_3$	−143.178	−143.885	−143.68

Fig. 1 Compressibility curves for $SrTiO_3$, $CaTiO_3$ and $BaTiO_3$.

however, if these potentials behave properly, this difference should be small. To test this, a set of calculations was made in which the system was allowed to relax from the experimental structure to the closest local energy minimum, by allowing the atomic coordinates to change and keeping the cell parameters constant at their experimental values. In the case of $SrTiO_3$, this relaxation did not lead to a noticeable modification of the atomic coordinates or lattice energy. In the cases of $CaTiO_3$ and $BaTiO_3$, although the relaxation led to a lowering of the lattice energy (Table 3), there was no substantial change in the structures.

An additional test for the quality of the potentials was made by comparing the calculated energy values for the experimental structures with those calculated from a Born–Haber cycle (U_{B-H}). The results are given in Table 3 and show an agreement within 4%.

All these results show that the potentials obtained from the binary compounds AO and TiO_2 (rutile) behave well to predict the structures of the ternary compounds $ATiO_3$.

3 Simulated annealing method

As long as we consider that the potentials have the correct behaviour, we can assume that the configuration that yields the minimum value for the cost function corresponds to the arrangement of atoms in the real structure. The problem of solving the structure then reduces to that of finding the global minimum of the calculated lattice energy.

The global optimisation algorithm chosen is the so-called "simulated annealing" algorithm. Given a starting configura-

Table 4 Lattice energy per formula for the structures obtained from simulated annealing runs for $CaTiO_3$. U_{corr} corresponds to the correct structure; U_{1perm}, to the structure with one permutation of Ti^{4+} by Ca^{2+}; U_{2perm}, to the structure with a double permutation of Ti^{4+} by Ca^{2+}; $U_{2perm'}$, to the structure with a double permutation of Ti^{4+} by Ca^{2+} with O^{2-} far from their correct positions and U_{uncorr}, to the uncorrelated structure with the lowest energy

Calculated without symmetry				Calculated with symmetry	
U_{corr}/ eV	U_{1perm}/ eV	U_{2perm}/ eV	$U_{2perm'}$/ eV	U_{corr}/ eV	U_{uncorr}/ eV
−149.225	−147.900	−147.388	−146.643	−149.365	−147.775

tion n, a trial one ($n + 1$) is chosen at random following certain rules. If the lattice energy of the trial configuration, V_{n+1}, is lower than or equal to V_n, then the new configuration is accepted. If V_{n+1} is greater than V_n, the new configuration is accepted according to a transition probability defined as $\exp(-\Delta V/kT)$, where $\Delta V = V_{n+1} - V_n$. This is known as the Metropolis importance-sampling algorithm. The temperature T is reduced after a certain number of steps. The cooling algorithm used is defined by $T_{n+1} = aT_n$, with $0.8 < a < 1$.

It must be noted that at a finite temperature the system has a finite probability of surmounting a potential barrier, and that the lower the temperature, the lower is that probability; so that as the temperature reduces the system should be confined to the global minimum.

All of the calculations were performed using a code developed by us.[9]

4 Simulated annealing results

4.1 Without symmetry restrictions

In this case, for all the compounds the runs were carried out considering that all atomic coordinates are independent of each other (space group $P\bar{1}$).

4.1.1 Results for $SrTiO_3$. We considered first $SrTiO_3$, which has the simplest structure among the three compounds. We obtained the correct structure in 40 out of 40 runs. The atomic coordinates are in agreement with the correct structure to the fourth decimal figure.

4.1.2 Results for $CaTiO_3$. In the case of $CaTiO_3$, the correct structure (Fig. 2a) was obtained two times over a total of 40 runs. However, the analysis of the incorrect structures showed that all of them were closely related to the correct one. In 28 of them the exchange of one Ti^{4+} ion by one Ca^{2+} ion was observed (one permutation) (Fig. 2b) and the exchange of two Ti^{4+} ions by two Ca^{2+} ions was observed in three of them (two permutations) (Fig. 2c). These permutations were also observed by Woodley et al.[3] The remaining three structures also have the permutation of two Ti^{4+} ions by two Ca^{2+} ions (two permutations') (Fig. 2d); however, O^{2-} ions were far away from their correct positions. The problem seems to be related to the characteristics of the present potentials at short distances, where the different ionic radii of Ca^{2+} and Ti^{4+} are not accounted properly. This is understandable on the basis that the interatomic potentials are more reliable in the neighbourhood of the equilibrium distances. However, it is worth mentioning that from all the obtained structures, the closest to the experimental one is that exhibiting the lowest lattice energy (Table 4). This fact shows that the potentials are reliable for the prediction of the global minimum, and that our current limitation is rather the simulated annealing procedure.

4.1.3 Results for $BaTiO_3$. For $BaTiO_3$ we did not obtain the correct structure in any of the 40 runs. No cation permutations
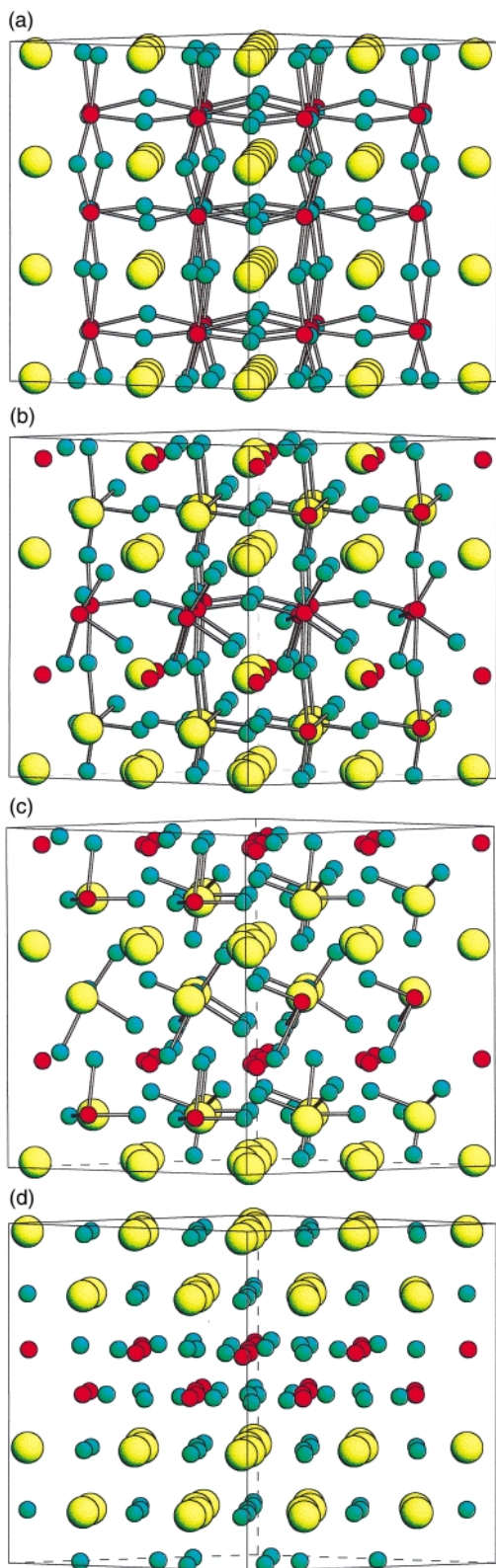
Fig. 2 Calculated structures for $CaTiO_3$ viewed along the $(1\bar{1}0)$ direction: (a) is the correct one, (b) presents the exchange of one Ti^{4+} ion by one Ca^{2+} ion, (c) presents the exchange of two Ti^{4+} ions for Ca^{2+} ions, and (d) also presents the exchange of two Ti^{4+} ions for Ca^{2+} ions but with O^{2-} ions far from their correct positions. Small cyan spheres represent O^{2-} ions, small red spheres represent Ti^{4+} ions and large yellow spheres represent Ca^{2+} ions.

Table 5 Lattice energy per formula for the structures obtained from simulated annealing runs for $BaTiO_3$. U_{corr} corresponds to the correct structure; U_{lowest}, to the structure with the lowest energy and U_{uncorr}, to the uncorrelated structure with the lowest energy

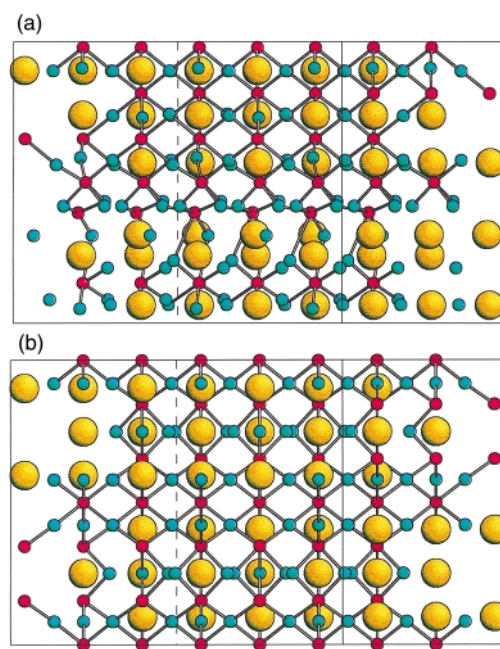| Calculated without symmetry		Calculated with symmetry	
U_{lowest}/eV	U_{uncorr}/eV	U_{corr}/eV	U_{uncorr}/eV
−143.033	−142.92	−143.81	−142.70

Fig. 3 Lowest energy structure obtained for $BaTiO_3$ with no symmetry imposition (a), and the crystallographic structure of $BaTiO_3$ (b) viewed along the (210) direction. Although structure (a) is not the correct one, a large portion of the unit cell resembles that of the real structure. Small cyan spheres represent O^{2-} ions, small red spheres represent Ti^{4+} ions and large orange spheres represent Ba^{2+} ions.

were observed in this case. Comparison of the lowest energy of these 40 runs (U_{lowest}, Table 5) with the calculated energy of the crystallographic structure (see Table 3) shows a small difference. An analysis of the structure with the lowest energy (Fig. 3a), which was obtained for 3 out of 40 runs, shows that a large portion of the unit cell resembles that of the real structure (Fig. 3b). The rest of the structures show no correlation with the real one and show energies above −142.92 eV.

4.2 With symmetry restrictions

Although the space group cannot always be determined unambiguously from powder diffraction, the presence of certain space symmetry elements such as screw axes, glide planes or centring (I, F, C, *etc.*) can often be detected from an analysis of the systematic absences in a powder diffraction pattern. We have previously shown that the imposition of symmetry restrictions arising from the presence of one these symmetry elements can improve the efficiency of the global optimisation procedure.[1]

4.2.1 Results for CaTiO₃. A new set of runs was carried out imposing the glide plane *a* (space group = *Pnma*). A remarkable increase in the efficiency of the global optimisation was obtained under these conditions. The correct structure was now obtained in 27 out of 40 runs, compared with 2 out of 40 obtained without symmetry restrictions, besides, the structures with permutations were completely absent. This can be explained taking into account that in this case not all the atomic coordinates are independent of each other. This avoids the permutation of atoms present in the former runs, since they are not consistent with the imposed symmetry restrictions. In other words, false minima with permutations of atoms are

Table 6 Atomic coordinates: experimental and calculated with and without symmetry for $CaTiO_3$ (orthorhombic, $a = 5.38$, $b = 5.44$, $c = 7.639$ Å)

	Experimental			Calculated without symmetry			Calculated with symmetry		
	x/a	y/b	z/c	x/a	y/b	z/c	x/a	y/b	z/c
Ti(1)	0.00000	0.50000	0.00000	0.00000	0.50000	0.00000	0.00000	0.50000	0.00000
Ti(2)	0.50000	0.00000	0.00000	0.51422	0.00073	0.00142	0.50000	0.00000	0.00000
Ti(3)	0.50000	0.00000	0.50000	0.51488	0.99807	0.52346	0.50419	0.99803	0.50519
Ti(4)	0.00000	0.50000	0.50000	0.99886	0.49562	0.52524	−0.00419	0.49803	0.50519
Ca(1)	0.00648	0.03560	0.25000	0.02397	0.00393	0.26240	−0.00812	0.01310	0.26156
Ca(2)	0.49352	0.53560	0.25000	0.49244	0.50420	0.26038	0.50812	0.51310	0.26156
Ca(3)	0.50648	0.46440	0.75000	0.50129	0.49050	0.76341	0.49471	0.49072	0.75792
Ca(4)	−0.01084	0.96440	0.75000	0.01608	0.98839	0.76261	0.00529	0.99072	0.75792
O(1)	0.57110	0.98390	0.25000	0.57755	0.98716	0.26252	0.52840	0.99718	0.25126
O(2)	−0.07110	0.48390	0.25000	−0.06474	0.48706	0.26434	−0.02840	0.49718	0.25126
O(3)	0.07110	0.51610	0.75000	0.07848	0.51108	0.76449	0.01690	0.50710	0.74874
O(4)	0.42890	0.01610	0.75000	0.43581	0.01341	0.76176	0.48310	0.00710	0.74874
O(5)	0.71030	0.71120	0.53730	0.73148	0.72281	0.56082	0.71054	0.71110	0.50906
O(6)	−0.21030	0.21120	0.53730	−0.21779	0.22448	0.55975	−0.21054	0.21110	0.50906
O(7)	0.28970	0.28880	0.03730	0.28617	0.27910	0.03821	0.28716	0.29091	0.01004
O(8)	0.21030	0.78880	0.03730	0.22480	0.78108	0.03848	0.21284	0.79091	0.01004
O(9)	0.71030	0.71120	0.96270	0.72767	0.72580	0.96750	0.71568	0.71938	0.98512
O(10)	−0.21030	0.21120	0.96270	−0.21542	0.22587	0.96577	−0.21568	0.21938	0.98512
O(11)	0.21030	0.78880	0.46270	0.22955	0.77531	0.48519	0.21088	0.78438	0.49706
O(12)	0.28970	0.28880	0.46270	0.28478	0.27607	0.48333	0.28912	0.28438	0.49706

avoided in this new configuration space. This imposition not only increases the efficiency but also leads to a more accurate set of atomic coordinates, as compared with the experimental ones (see Table 6). The energy value of the correct structure (U_{corr}) and the lowest energy among the ones not showing correlation with the correct structure (U_{uncorr}) are shown in Table 4. As in the case without symmetry restrictions, the structure closest to the experimental one is that exhibiting the lowest energy.

4.2.2 Results for BaTiO$_3$. For $BaTiO_3$ a set of 40 runs was carried out imposing the glide plane c (space group = $P6_3/mmc$). The correct structure was then obtained in 18 out of 40 runs compared with 0 out of 40 runs obtained with no symmetry restrictions. Similarly to the case for $CaTiO_3$, the structure closest to the experimental one is that exhibiting the lowest energy (Table 5). This specific case shows that the imposition of symmetry restrictions can make the difference between solving and not solving a compound with this complexity. Atomic coordinates are very accurate compared with those of the correct one (not shown). Accuracy of atomic coordinates might be crucial for structure refinement by Rietveld analysis.

5 Rietveld refinement

5.1 Choosing a starting model

In order to emulate the usual procedure to solve an unknown structure from powder diffraction data and an annealing run, and to show that the structural models obtained from our annealing runs are good for Rietveld analysis, we perform refinements using the set of atomic coordinates obtained in these runs as a starting model. We use calculated neutron or X-ray powder diffractograms as the "experimental" data. For this purpose we use FULLPROF.[10] Profile parameters were selected from those obtained in real refinements of similar compounds performed in our laboratory[11,12] and the structural models were obtained from the literature.[6–8]

5.2 Refinements

In a first step, a FULLPROF run was performed using zero refined parameters, in order to check the starting models and obtain their initial R_{wp} and R_{Bragg} values. In a second step, Rietveld refinements were performed until the best R_{wp} and R_{Bragg} values were obtained. In every case it was assumed

Table 7 R_{Bragg} and R_{wp} (%) obtained from X-ray Rietveld refinement of structures calculated for $CaTiO_3$ with no symmetry restrictions

XRD data	R_{Bragg}, initial	R_{Bragg}, final	R_{wp}, initial	R_{wp}, final
Correct	18.98	2.93	123	4.77
1 Permutation	45.33	3.96	170	6.95
2 Permutations	52.25	3.88	153	6.43
2 Permutations′	44.8	2.96	807	4.79

Table 8 R_{Bragg} and R_{wp} (%) obtained from neutron Rietveld refinement of structures calculated for $CaTiO_3$ with no symmetry restrictions

Neutron data	R_{Bragg}, initial	R_{Bragg}, final	R_{wp}, initial	R_{wp}, final
Correct	52.15	0.0325	102	0.145
1 Permutation	81.27	43.65	138	60.1
2 Permutations	104.02	71.03	178	81.8
2 Permutations′	107.49	65.76	359	83.6

that the space group was unknown and the refinements were performed in $P\bar{1}$.

Since for $SrTiO_3$ the calculated atomic coordinates are in agreement with the real ones to the fourth decimal figure, we consider this a refined structural model and no Rietveld refinements were performed.

5.2.1 Results for CaTiO$_3$. *5.2.1.1 Structural models obtained without symmetry restrictions.* In this case we divide our results into four subgroups, *i.e.* the "correct structure", one permutation, two permutations (with oxygens close to their correct positions) and two permutations′ (with oxygens far from their correct positions).

The corresponding R_{wp} and R_{Bragg} values for each subgroup are shown in Table 7. As expected, the best R values are obtained with the "correct structure". $CaTiO_3$ is a "hard to solve" case for the specific problem of the cation permutations when XRD data are used since Ca^{2+} and Ti^{4+} are isoelectronic and consequently their atomic scattering factors are very similar. This is clearly observed when the final R_{wp} and R_{Bragg} values are compared. The only solution to this problem is to use neutron diffraction, because of the very different values for the scattering lengths of Ca and Ti. The results are shown in

Table 9 R_{Bragg} and R_{wp} (%) obtained from Rietveld refinement of structures calculated for $CaTiO_3$ with symmetry restrictions

		R_{Bragg}, initial	R_{Bragg}, final	R_{wp}, initial	R_{wp}, final
XRD data	Correct	22.37	2.98	45.3	4.53
	Uncorrelated	32.91	19.64	112	39.3
ND data	Correct	68.27	0.0298	113	0.144
	Uncorrelated	99.41	59.03	262	73.0

Table 10 R_{Bragg} and R_{wp} (%) obtained from Rietveld refinement of structures calculated for $BaTiO_3$ without symmetry restrictions

		R_{Bragg}, initial	R_{Bragg}, final	R_{wp}, initial	R_{wp}, final
XRD data	Related	39.48	34.63	123	108
	Uncorrelated	49.23	45.14	141	134
ND data	Related	82.30	57.45	284	72.1
	Uncorrelated	112.8	87.85	354	85.6

Table 11 R_{Bragg} and R_{wp} (%) obtained from Rietveld refinement of structures calculated for $BaTiO_3$ with symmetry restrictions

		R_{Bragg}, initial	R_{Bragg}, final	R_{wp}, initial	R_{wp}, final
XRD data	Correct	22.5	0.494	38.4	0.916
	Uncorrelated	46.30	42.51	131	114
ND data	Correct	41.6	0.084	70.6	0.267
	Uncorrelated	99.9	63.80	319	78.7

Table 8. Clearly only the correct structure gives a good solution. As it can be observed, some R values are abnormally low. This is due to the fact that we have used calculated diffractograms as "experimental" ones; thus, the fit is very good (especially in the neutron case) giving these extremely low values.

5.2.1.2 Structural models obtained with symmetry restrictions. In this case only two subgroups are distinguished, *i.e.*, the "correct structure" and the ones without any correlation with the correct structure. No permutations were observed. Initial and final R_{wp} and R_{Bragg} values for XRD and ND (neutron diffraction) are shown in Table 9. Clearly, only the correct structure gives reasonably good final values.

5.2.2 Results for $BaTiO_3$. *5.2.2.1 Structural models obtained without symmetry restrictions.* Although in this case the correct structure was not obtained, two subgroups may be distinguished, *i.e.* the structure in which a large portion of the unit cell resembles that of the real structure, and the ones that show no correlation with the correct structure. Initial and final R_{wp} and R_{Bragg} values for XRD and ND are shown in Table 10. We did not obtain good final values as expected.

5.2.2.2 Structural models obtained with symmetry restrictions. In this case only two subgroups are distinguished, *i.e.*, the "correct structure" and the ones without any correlation with the correct structure. No permutations were observed. Initial

and final R_{wp} and R_{Bragg} values for XRD and ND are shown in Table 11. Clearly, only the correct structure gives good final values.

6 Conclusions

We have shown that the interatomic potentials obtained for binary compounds are very good for the prediction of the structures of ternary compounds using simulated annealing with only the incorporation of the potential energy to the cost function. A tremendous increase in the efficiency of obtaining the correct structure and in the accuracy of the atomic co-ordinates could be obtained by incorporation of the space symmetry elements obtainable from powder diffraction. In the case of complex structures like, for example, hexagonal $BaTiO_3$, the incorporation of symmetry elements is crucial for the prediction of the correct structure. On the other hand, without ways to select proper symmetry elements, the correct structure could still be very hard to predict. To the best of our knowledge, this is the first time a structure of the complexity of $BaTiO_3$ has been solved with the lone incorporation of the interatomic potentials in the cost function.

8 References

1 L. Reinaudi, R. E. Carbonio and E. P. M. Leiva, *Chem. Commun.*, 1998, 255.
2 J. Pannetier, J. Bassas-Alsina, J. Rodriguez-Carbajal and V. Caignaert, *Nature*, 1990, **346**, 343.
3 S. M. Woodley, P. D. Battle, J. D. Gale and C. R. A. Catlow, *Phys. Chem. Chem. Phys.*, 1999, **1**, 2535.
4 H. Putz, J. C. Schön and M. Jansen, *J. Appl. Crystallogr.*, 1999, **32**, 864.
5 C. M. Freeman, J. M. Newsam, S. M. Levine and C. R. A. Catlow, *J. Mater. Chem.*, 1993, **3**, 351.
6 Yu. A. Abramov, V. G. Tsirelson, V. E. Zavodnik, S. A. Ivanov and I. D. Brown, *Acta Crystallogr.*, Sect. B, 1995, **51**, 942.
7 A. Beran, E. Libowitzky and T. Armbruster, *Can. Mineral.*, 1996, **34**, 803.
8 J. Akimoto, Y. Gotoh and Y. Oosawa, *Acta Crystallogr.*, Sect. C, 1994, **39**, 160.
9 The code, compiled for the Windows, Linux and Alpha-Unix platforms, is available upon request at: carbonio@fisquim.fcq.unc.edu.ar.
10 J. Rodriguez-Carbajal, *Physica B*, 1993, **192**, 55.
11 V. Nassif, R. E. Carbonio and J. A. Alonso, *J. Solid State Chem.*, 1999, **146**, 266.
12 H. Falcón, A. E. Goeta, G. Punte and R. E. Carbonio, *J. Solid State Chem.*, 1997, **133**, 379.
13 C. R. A. Catlow, C. M. Freeman and R. L. Royle, *Physica B*, 1985, **131**, 1.
14 G. V. Lewis, *Physica B*, 1985, **131**, 114.